

# Supporting Information

Rahmeh et al. 10.1073/pnas.1209147109

## SI Materials and Methods

**Protein Expression and Purification.** L was expressed in Sf21 cells with an N-terminal 6xHis tag and purified by Ni-nitrilotriacetic acid (NTA) affinity, followed by MonoS chromatography as described previously (1). N-RNA was isolated from purified vesicular stomatitis virus (VSV) as described previously (2), with an additional passage on the CsCl gradient. P, P<sub>N<sub>NTD</sub></sub>, and P<sub>N<sub>NTD</sub></sub> deletions were cloned with N-terminal 6xHis-ENLYFQSN<sub>A</sub> in a modified pET16 vector. [The underlined residues indicate the tobacco etch virus (TEV) protease recognition motif; cleavage by TEV occurs between Q and S.] P and N-terminal P deletions were cloned with an N-terminal 6xHis-GSS-(maltose binding protein)-ENLYFQSGSGG. The plasmids were transformed in BL21 (DE3) *Escherichia coli*. The cells were grown in LB containing 100 µg/mL of ampicillin and induced at an A<sub>600</sub> of 0.6 with 1 mM isopropyl β-D-thiogalactopyranoside for 4 h at 30 °C. All fragments were first purified by Ni-NTA agarose chromatography (Qiagen) following the manufacturer's standard protocol with gradient elution. To remove the N-terminal tags, proteins were dialyzed in 20 mM Tris-HCl (pH 7.4), 250 mM NaCl, and 25 mM imidazole and incubated with a 1:20 mass ratio of 6xHis-tagged TEV:protein overnight at 4 °C. The cleaved proteins were separated from free maltose-binding protein (MBP) and TEV by a second round of Ni-NTA purification, in which they eluted in the flow-through fraction. The cleaved proteins were dialyzed in 20 mM Tris (pH 7.4), 150 mM NaCl, and 1 mM DTT.

**Size-Exclusion Chromatography.** Here 120 µg of L and 24.5 µg of P<sub>N<sub>NTD</sub></sub> were individually passed through a Superdex 200 HR 10/30 column (GE Healthcare) or, alternatively, first mixed together for 1 h on ice before column passage. The column was run at 0.25 mL/min, and 250-µL fractions were collected. Apparent molecular weights were extrapolated from a standard curve calculated from the elution volumes of a gel filtration standard (BioRad).

**EM and Image Processing.** Micrographs were collected using a Tecnai T12 electron microscope (FEI) equipped with an LaB<sub>6</sub> filament and operated at an acceleration voltage of 120 kV. Micrographs were recorded on imaging plates at a magnification of 67,000× and a defocus of approximately -1.5 µm using low-dose procedures. For the L-P<sub>N<sub>NTD</sub></sub> deletion complexes, two independent datasets were recorded. Imaging plates were read with a scanner (DITABIS) using a step size of 15 µm, a gain

setting of 20,000, and a laser power setting of 30%; 2 × 2 pixels were averaged to yield a pixel size of 4.5 Å at the specimen level (3). BOXER, part of the EMAN software package (4), was used to interactively select particles. For the L + P<sub>N<sub>NTD</sub></sub> sample, 5,842 particles were selected from 54 images. For the L + P41-106 sample, 4,890 particles were selected from 28 images for the first dataset and 3,950 particles were selected from 36 images for the second dataset. For the L + P61-106 sample, 4,028 particles were selected from 39 images for the first dataset and 3,826 particles were selected from 39 images for the second dataset. For the L + P81-106 sample, 3,615 particles were selected from 26 images for the first dataset and 2,541 particles were selected from 39 images for the second dataset. For the L + P1-80 sample, 2,150 particles were selected from 21 images for the first dataset and 2,325 particles were selected from 37 images for the second dataset. For the L + P1-80 + P81-106 sample, 3,985 particles were selected from 38 images for the first dataset and 2,465 particles were selected from 39 images for the second dataset. All particles were windowed into 64 × 64-pixel images and classified using the SPIDER software package (5). The particles were rotationally and translationally aligned and subjected to 10 cycles of multireference alignment. Each round of multireference alignment was followed by *k*-means classification into 20 classes. The references used for the first multireference alignment were chosen at random from the particle images.

**Ni-NTA Pulldown Assay.** Here 3 µg (12.5 pmol) of 6xHis-tagged L was incubated with 50 pmol of untagged P or P deletions in 300 µL of buffer containing 50 mM NaH<sub>2</sub>PO<sub>4</sub> (pH 7.4), 250 mM NaCl, and 10 mM imidazole for 1 h on ice, followed by the addition of 15 µL of Ni-NTA agarose beads (Qiagen) with end-to-end rotation for 1 h at 4 °C. The beads were precipitated by centrifugation at 2,000 × *g* for 3 min and then washed five times with 500 µL of binding buffer containing 30 mM imidazole. The beads were boiled in 2× SDS/PAGE loading buffer, and the proteins were separated by 4–12% SDS/PAGE. The precipitated bands were quantitated using ImageJ software.

**Western Blot Analysis.** A polyclonal antibody against P was generated by immunization of rabbits with His-P purified from *Escherichia coli* (Covance). Nitrocellulose membranes were probed using a 1:20,000 dilution of anti-P, followed by a 1:5,000 dilution of anti-rabbit HRP (Santa Cruz Biotechnology). Bands were visualized by ECL (Pierce) and quantified using an AlphaImager (Alpha Innotech).

1. Rahmeh AA, et al. (2010) Molecular architecture of the vesicular stomatitis virus RNA polymerase. *Proc Natl Acad Sci USA* 107:20075–20080.
2. Emerson SU, Yu Y (1975) Both NS and L proteins are required for in vitro RNA synthesis by vesicular stomatitis virus. *J Virol* 15:1348–1356.
3. Li Z, Hite RK, Cheng Y, Walz T (2010) Evaluation of imaging plates as recording medium for images of negatively stained single particles and electron diffraction patterns of two-dimensional crystals. *J Electron Microsc (Tokyo)* 59:53–63.

4. Ludtke SJ, Baldwin PR, Chiu W (1999) EMAN: Semiautomated software for high-resolution single-particle reconstructions. *J Struct Biol* 128:82–97.
5. Frank J, et al. (1996) SPIDER and WEB: Processing and visualization of images in 3D electron microscopy and related fields. *J Struct Biol* 116:190–199.

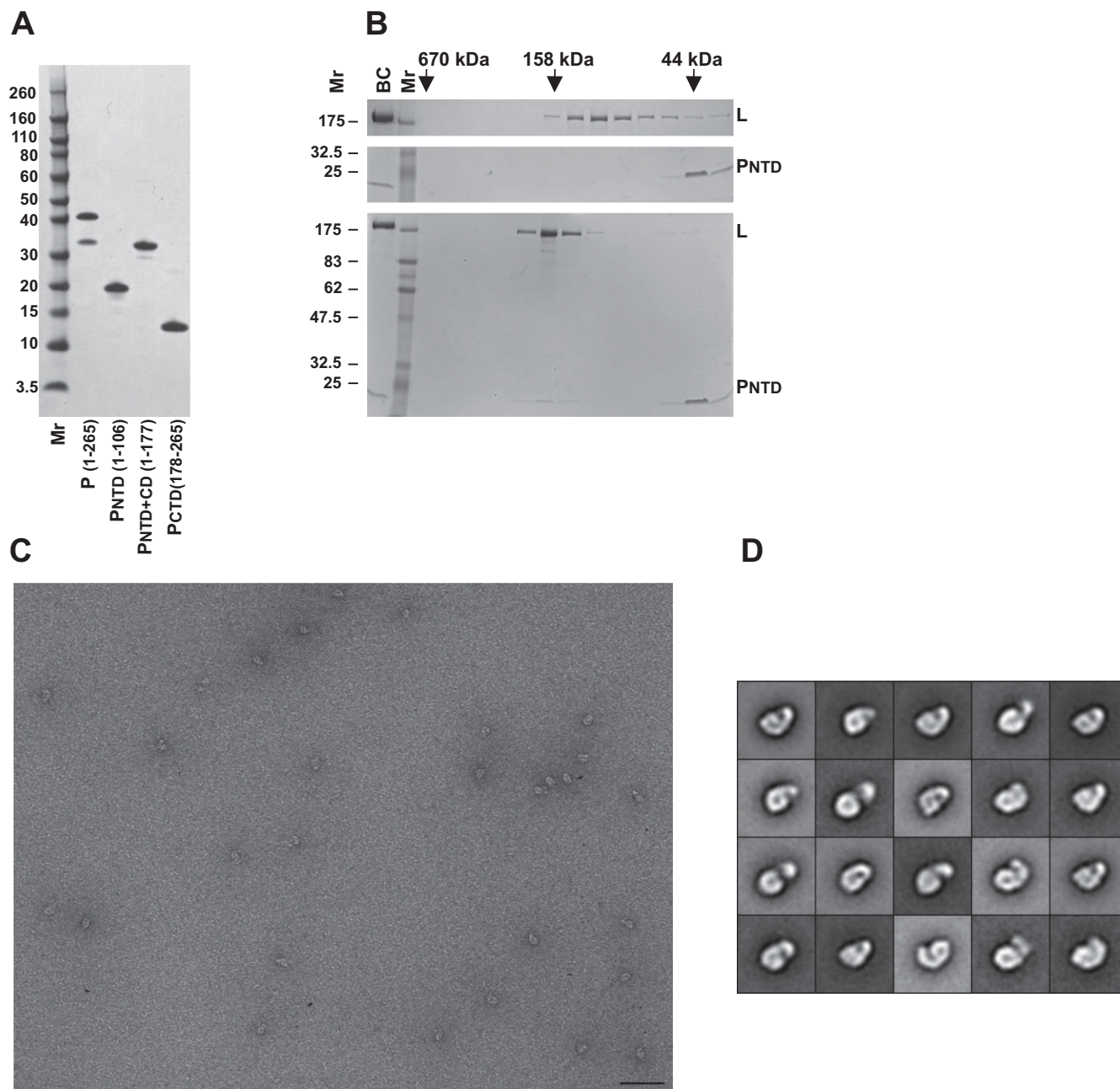


**Fig. S1.** Purification and EM characterization of an L-P<sub>N<sub>TD</sub></sub> complex. (A) Full-length P or fragments comprising P<sub>N<sub>TD</sub></sub> (1–106), P<sub>N<sub>TD</sub>+CD</sub> (1–177), or P<sub>CTD</sub> (178–265) were expressed in *E. coli* with a 6xHis-MBP tag. Proteins were purified, and the tag was cleaved off with TEV and separated by Ni-NTA chromatography. The purified proteins were analyzed by 4–12% SDS/PAGE and visualized with Coomassie blue staining. (B) Isolation of an L-P<sub>N<sub>TD</sub></sub> complex by size-exclusion chromatography. L (Top), P<sub>N<sub>TD</sub></sub> (Middle), and L + P<sub>N<sub>TD</sub></sub> (Bottom) were passed through a Superdex 200 column. The eluted fractions were analyzed by 4–12% SDS/PAGE and visualized with Coomassie blue staining. The elution of molecular weight standards is indicated by arrows. BC, before column; M<sub>r</sub>, molecular weight marker. (C) Representative EM image of L + P<sub>N<sub>TD</sub></sub> in a negative stain. (Scale bar: 50 nm.) (D) Class averages of single particles of the L-P<sub>N<sub>TD</sub></sub> complex obtained after classification of 5,842 particles into 20 classes. The side length of the individual panels is 29 nm.

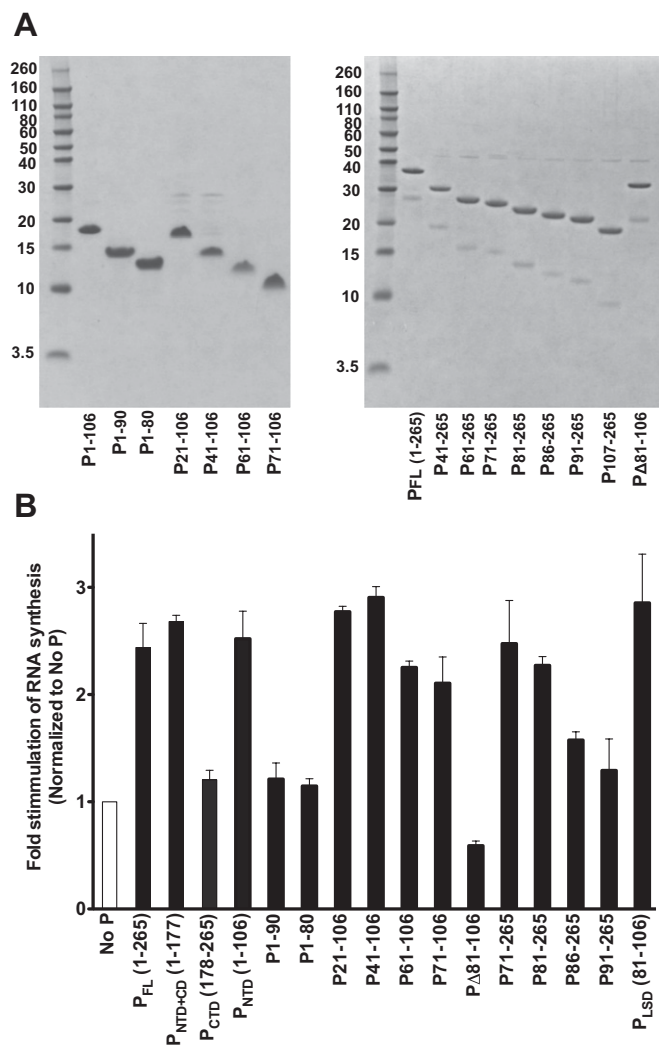


**Fig. S2.** Effects of  $P_{NTD}$  deletion mutants and N-terminal deletions of full-length P ( $P_{FL}$ ) on stimulation of L processivity on the Le19 template. (A) Series of deletion mutants spanning  $P_{NTD}$  (Left) and N-terminal deletions of  $P_{FL}$  (Right) were expressed and purified as in Fig. S1A. The purified proteins were separated by 4–12% SDS/PAGE and visualized with Coomassie blue staining. (B) Total amount of RNA synthesis on Le19 in the presence of each of the  $P_{NTD}$  deletion mutants and the N-terminal deletions of  $P_{FL}$  were quantified by summing the band intensities, normalized to levels of RNA synthesis produced in the absence of P, and graphed. Error bars represent the SD from the mean of two independent experiments.

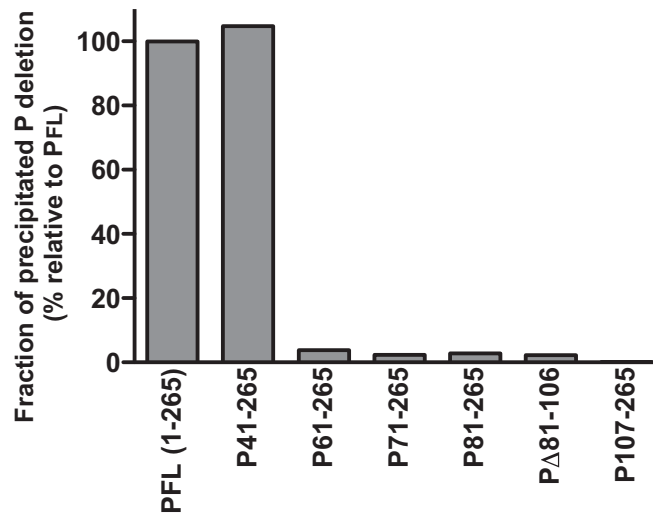


**Fig. S3.** Quantitation of the fraction of precipitated P deletions by L. The input and the precipitated bands of P<sub>FL</sub> and P deletions in Fig. 3 were quantitated, and the fraction of each precipitated band/input was calculated. The precipitated fractions of each deletion were normalized relative to that of P<sub>FL</sub> and graphed.



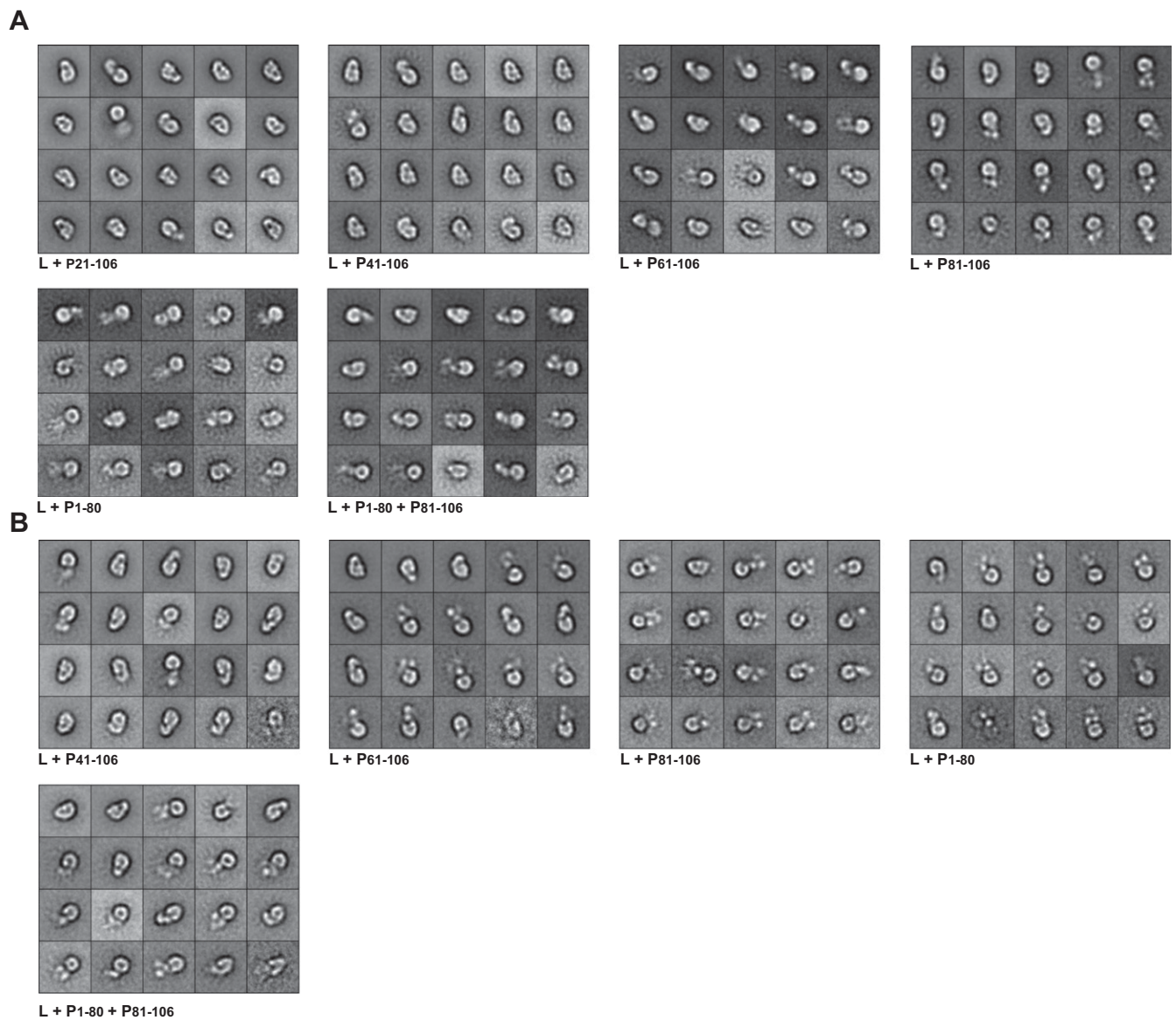


**Fig. 54.** Single-particle EM analysis of negatively stained L proteins mixed with a molar excess of  $P_{NTD}$  deletions. (A) Class averages of single particles obtained after classification into 20 classes of 4,302 particles for L + P21-106, 4,890 particles of L + P41-106, 4,028 particles of L + P61-106, 3,615 particles of L + P81-106, 2,150 particles of L + P1-80, and 3,985 particles of L + P1-80 + P81-106. (B) Class averages of single particles obtained in a second independent experiment after classification into 20 classes of 3,950 particles of L + P41-106, 3,826 particles of L + P61-106, 2,541 particles of L + P81-106, 2,325 particles of L + P1-80, and 2,465 particles of L + P1-80 + P81-106.

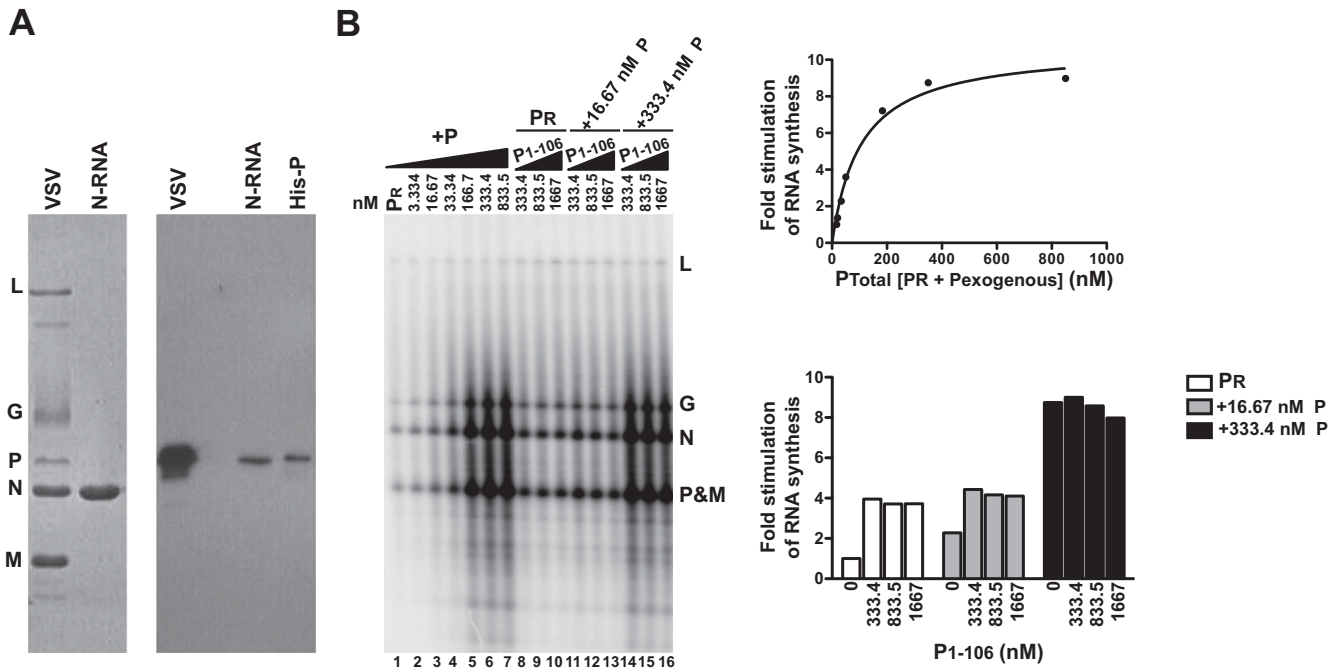


**Fig. 55.** Optimization of in vitro transcription conditions using an encapsulated *N*-RNA template. (A) Estimation of the amount of residual P remaining on the purified *N*-RNA. (Left) *N*-RNA was isolated from purified virus and visualized by Coomassie blue staining on low-Bis (0.13% Bis) 10% SDS/PAGE. (Right) The presence of residual P ( $P_R$ ) on *N*-RNA was detected by Western blot analysis using a polyclonal antibody against P, where 0.22 pmol  $P_R/\mu\text{g}$  of purified *N*-RNA were estimated by quantitation of the band intensity of 4  $\mu\text{g}$  of *N*-RNA relative to the band intensity of 0.8335 pmol of purified recombinant P using an Alphamager. (B) Measurement of the stimulation of transcription as a function of increasing concentrations of P and the effect of increasing concentrations of  $P_{NTD}$  in a range of P concentrations. (Left) Here 50- $\mu\text{L}$  in vitro transcription reactions were reconstituted with 5  $\mu\text{g}$  of *N*-RNA, 1  $\mu\text{g}$  (4.16 pmol) of L, and increasing concentrations of P (lanes 1–7). Transcription reactions were performed in the presence of [ $\alpha$ - $^{32}\text{P}$ ] GTP. The products were separated by electrophoresis on acid-agarose gels and analyzed with a PhosphorImager. The five VSV mRNAs P, M (matrix), N, G (glycoprotein), and L are shown to the right. (Right) (Upper) The total amount of synthesis was quantified by summing the band intensities, normalized to levels of RNA synthesis produced by  $P_R$ , and graphed. (Lower) Increasing concentrations of  $P_{NTD}$  were added to in vitro transcription reaction in the absence of exogenous P (lanes 8–10), or in the presence of suboptimal (lanes 11–13) or optimal (lanes 13–16) concentrations of P. RNA synthesis was analyzed as in A and graphed.

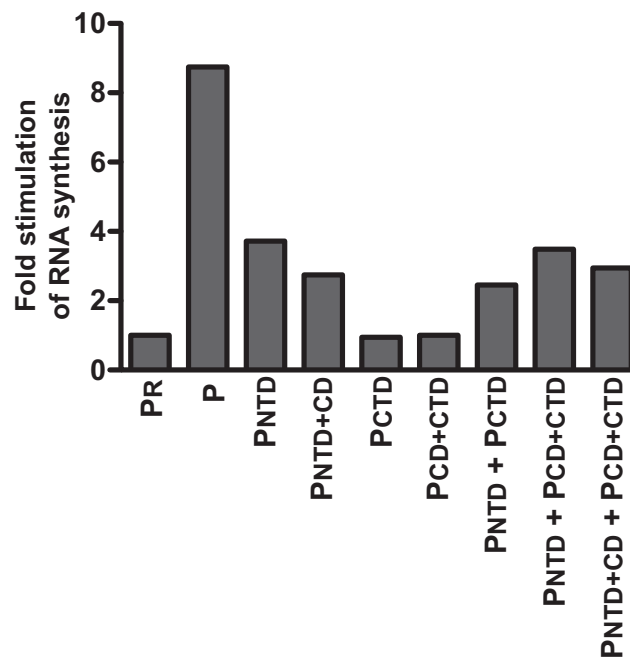


**Fig. 56.** Complementation analysis of the domains of P in transcription of an encapsulated *N*-RNA template. Here 50- $\mu\text{L}$  in vitro transcription reactions were reconstituted with 5  $\mu\text{g}$  of *N*-RNA, 1  $\mu\text{g}$  (4.16 pmol) of L, and 41.6 pmol (833.5 nM) each of  $P_{NTD}$ ,  $P_{NTD+CD}$ ,  $P_{CTD}$ , or  $P_{CD+CTD}$ , or a combination of  $P_{NTD}$  +  $P_{CTD}$ ,  $P_{NTD}$  +  $P_{CD+CTD}$ , or  $P_{NTD+CD}$  +  $P_{CD+CTD}$ . RNA synthesis was analyzed as in Fig. 55 and graphed.